Supporting Information

Ultrafast, Continuous and Shape-controlled Preparation of CeO_2 Nanostructures: nanorods and nanocubes in a Microfluidic System

Hongbao Yao[a], Yujun Wang[a,*1], Yu Jing [a,*2], Guangsheng Luo[a]

[a]*State Key Laboratory of Chemical Engineering, Department of Chemical Engineering, Tsinghua University, Beijing 100084, China*

Corresponding author*[1]: Tel: 86-10-62798447, Fax: 86-10-62770304

Email address: wangyujun@mail.tsinghua.edu.cn

Corresponding author*[2]: Tel: 86-10-62795335, Fax: 86-10-62770304

Email address: jingyuthu@163.com

1. SEAD pattern of different CeO_2 sample

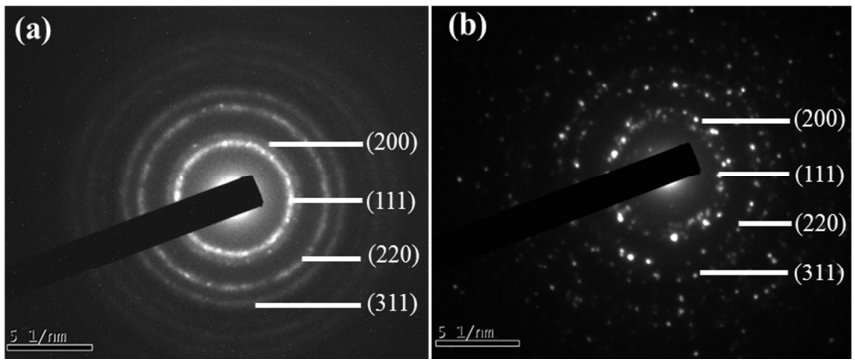

Fig. S1 SEAD pattern of (a) CeO_2_r, (b) CeO_2_c.

2. Comparison with CeO_2 nanorods prepared by different methods

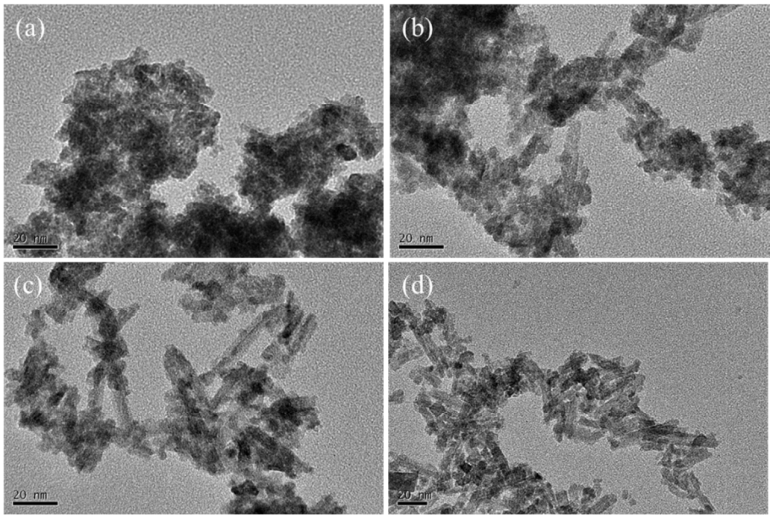

Fig. S2 TEM images of CeO_2 nanorods prepared under different reaction time using traditional hydrothermal methods: (a) 15 min, (b) 30 min, (c) 1 h, and (d) 2 h [reaction temperature: 150 °C, $Ce(NO_3)_3$ initial concentration: 0.05 mol/L, NaOH initial concentration: 2 mol/L].

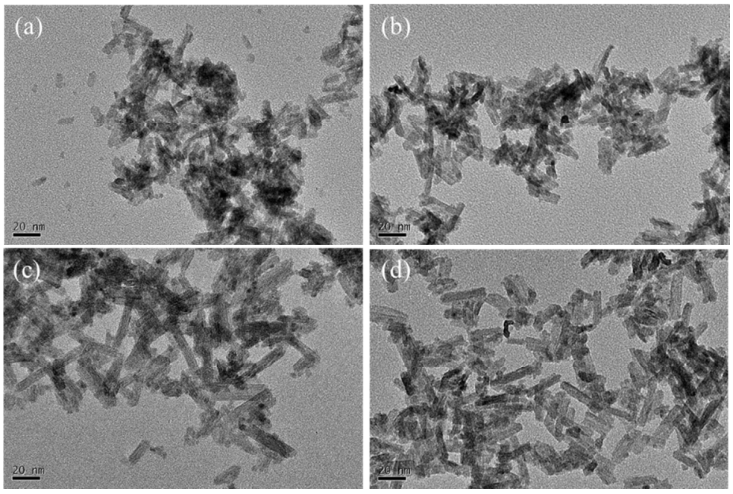

Fig. S3 TEM images of CeO_2 nanorods prepared under different reaction time using our microfluidic system: (a) 1 min, (b) 2 min, (c) 3.5 min, and (d) 8 min [reaction temperature: 150 °C, continuous phase: $Ce(NO_3)_3$, concentration: 0.05 mol/L; dispersed phase: NaOH, concentration: 2 mol/L, fixed phase ratio 1:1, flow rate changing from 5 mL/min to 20 mL/min to obtain different residence time].

3. TEM image of the CeO_2_np sample

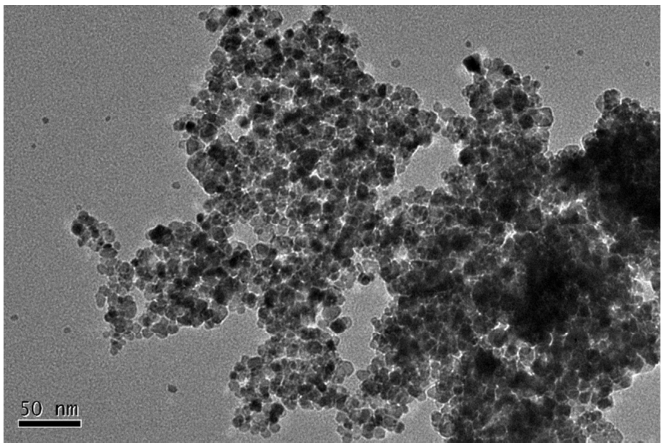

Fig. S4 TEM image of the CeO_2_np sample.

4. Determination of surficial Ce(III) concentration of CeO_2 based on XPS

It is generally considered that the deconvolution of the Ce 3d fine XPS spectrum could be labeled as two pairs of doublets (v_0/u_0 and v′/u′) and three pairs of doublets (v/u, v′′/u′′ and v′′′/u′′′), in which v^n and u^n refer to the $3d_{5/2}$ and $3d_{3/2}$ spin–orbit component of cerium ions,

respectively [1-4]. Accordingly, the peaks at ν_0, ν', u_0 and u' (880.4, 885.5, 898.8, 903.7±0.7 eV) represent the presence of Ce^{3+}, while the characteristic peaks of Ce^{4+} are located at ν, ν'', ν''', u, u'' and u''' (882.7, 888.96, 898.2, 901.3, 907, 916.7±0.7 eV) [5-7].

Thus, the relative Ce^{3+} concentration in the catalysts can be determined by calculating the relative integrated area ratios based on Equation (S1):

$$[Ce^{3+}] = \frac{A_{\nu'} + A_{\nu_0} + A_{u'} + A_{u_0}}{A_{\nu'} + A_{\nu_0} + A_{u'} + A_{u_0} + A_{\nu''} + A_{\nu'''} + A_{u''} + A_{u'''}} \quad (S1)$$

where A_i is the integration area of peak "i".

5. O1s XPS spectra of CeO_2_np, CeO_2_nr and CeO_2_nc samples

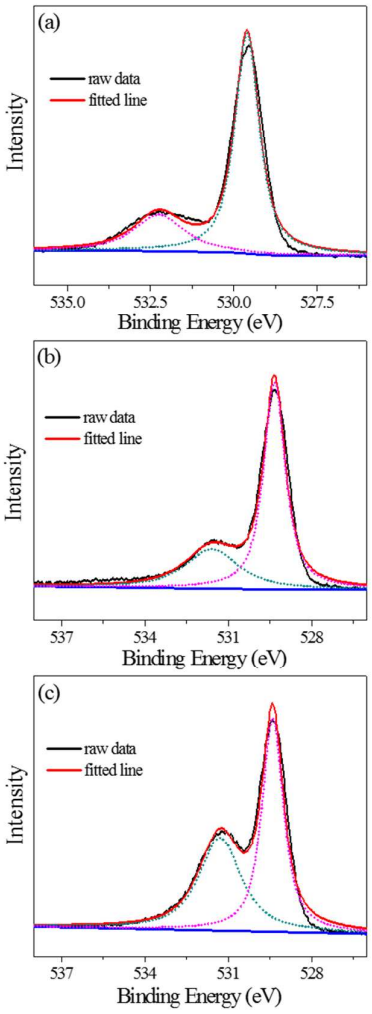

Fig. S5 O1s XPS spectra of (a) CeO_2_np, (b) CeO_2_nr and (c) CeO_2_nc, respectively.

6. Computational details

All calculations presented in this work were carried out at the DFT+U level using the Materials Studio program. Projector-augmented wave (PAW) method was employed to describe the interactions between the atomic core and valence electrons (i.e., 5s, 5p, 5d, $4f$ and 6s electrons for Ce atoms, and 2s and 2p for O atoms) with a kinetic energy cutoff of 500 eV [8, 9]. The exchange correlation functional is the generalized gradient approximation, GGA, of Perdew and Wang, PW91[10]. A U value of 5.0 eV was selected based on previous theoretical studies[11, 12].

The (111), (110), and (100) surfaces were modeled as (2×2) periodically repeated slabs consisting of 12, 7, and 9 atomic layers, respectively, separated by 15 Å of vacuum space to prevent unphysical interactions between the slab and its periodic images perpendicular to the surface[13]. Fig. S4 shows the models used for bulk CeO_2, (111), (110) and (100) surface systems, respectively. Oxygen vacancies were generated on both sides of the slab to ensure that the slab has no net dipole. The total oxygen vacancy formation energy (E_{vac}) was defined as:

$$E_{vac} = E_{slab/vac} - E_{slab} + \frac{1}{2n} E_{O_2}$$

Where E_{slab} is the total energy of the slab, $E_{slab/vac}$ is the total energy of the slab with oxygen atoms partially removed, E_{O_2} is the total energy of a gas phase O_2 molecule and n is the mumber of oxygen atoms removed.

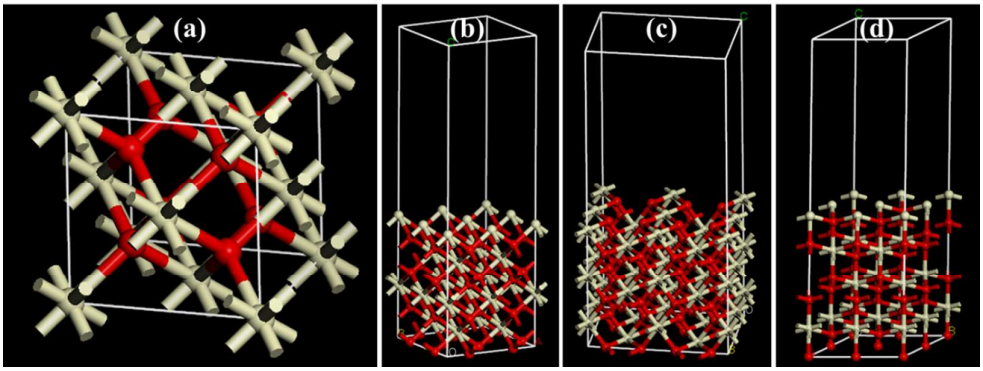

Fig. S6 models used for (a) bulk CeO_2, (b) (100), (c) (110) and (d) (111) surface systems, respectively.

Reference

1. Holgado, J. P.; Alvarez, R.; Munuera, G., Study of CeO_2 XPS spectra by factor analysis: reduction of CeO_2. *Appl. Surf. Sci.* **2000,** 161, (3-4), 301-315.

2. Korsvik, C.; Patil, S.; Seal, S.; Self, W. T., Superoxide dismutase mimetic properties exhibited by vacancy engineered ceria nanoparticles. *Chem. Commun.* **2007**, (10), 1056-1058.

3. Dutta, P.; Pal, S.; Seehra, M. S.; Shi, Y.; Eyring, E. M.; Ernst, R. D., Concentration of Ce^{3+} and oxygen vacancies in cerium oxide nanoparticles. *Chem. Mater.* **2006,** 18, (21), 5144-5146.

4. Watanabe, S.; Ma, X.; Song, C., Characterization of Structural and Surface Properties of Nanocrystalline TiO_2-CeO_2 Mixed Oxides by XRD, XPS, TPR, and TPD. *J. Phys. Chem. C* **2009,** 113, (32), 14249-14257.

5. Paparazzo, E.; Ingo, G. M.; Zacchetti, N., X-ray-induced reduction effects at CeO_2 surfaces - an x-ray photoelectron-spectroscopy study. *J. Vac. Sci. Technol., A* **1991,** 9, (3), 1416-1420.

6. Mullins, D. R.; Overbury, S. H.; Huntley, D. R., Electron spectroscopy of single crystal and polycrystalline cerium oxide surfaces. *Sur. Sci.* **1998,** 409, (2), 307-319.

7. Kumar, A.; Babu, S.; Karakoti, A. S.; Schulte, A.; Seal, S., Luminescence Properties of Europium-Doped Cerium Oxide Nanoparticles: Role of Vacancy and Oxidation States. *Langmuir* **2009,** 25, (18), 10998-11007.

8. Yin, L.-L.; Lu, G.; Gong, X.-Q., A DFT plus U study on the oxidative chlorination of CH4 at ceria: the role of HCl. *Catal. Sci. Technol.* **2017,** 7, (12), 2498-2505.

9. Yang, Z. X.; Woo, T. K.; Baudin, M.; Hermansson, K., Atomic and electronic structure of unreduced and reduced CeO_2 surfaces: A first-principles study. *J. Chem. Phys.* **2004,** 120, (16), 7741-7749.

10. Canadell, E., *Electronic Structure of Solids*. John Wiley & Sons, Ltd: 2006; p 293-309.

11. Capdevila-Cortada, M.; Garcia-Melchor, M.; Lopez, N., Unraveling the structure sensitivity in methanol conversion on CeO_2: A DFT + U study. *J. Catal.* **2015,** 327, 58-64.

12. Nolan, M.; Parker, S. C.; Watson, G. W., The electronic structure of oxygen vacancy defects at the low index surfaces of ceria. *Surf. Sci.* **2005,** 595, (1), 223-232.

13. Nolan, M.; Grigoleit, S.; Sayle, D. C.; Parker, S. C.; Watson, G. W., Density functional theory studies of the structure and electronic structure of pure and defective low index surfaces of ceria. *Surf. Sci.* **2005,** 576, (1-3), 217-229.